Journal of Thermal Analysis and Calorimetry (2022) 147:7855–7864
https://doi.org/10.1007/s10973-021-11073-x

Hybrid pseudo-direct numerical simulation of high Rayleigh number flows up to 10^{11}

Alexander Nee[1] · **Ali J. Chamkha**[2,3]

Received: 16 January 2021 / Accepted: 10 September 2021 / Published online: 9 October 2021

Abstract

This paper examines the capability of hybrid lattice Boltzmann method to simulate developed turbulent buoyancy-driven flows in closed rectangular cavities. The two-relaxation time mesoscopic lattice Boltzmann method is used as a fluid dynamics solver, whereas the thermal behavior is described in terms of the macroscopic energy equation. Numerical simulation is performed for air-filled square and tall cavities in a range of the Rayleigh number $10^9 \le Ra \le 10^{11}$. An in-house numerical code is developed in this study and successfully validated against up-to-date numerical and experimental data of other researches. It is found that the proposed hybrid approach accurately predicts the location of thermal plumes at the isothermal walls despite an insignificant error in the heat transfer rate with the $Ra \ge 3 \cdot 10^{10}$.

Keywords Turbulent natural convection · Hybrid lattice Boltzmann · Two-relaxation time · Direct numerical simulation

Abbreviations

a	Thermal diffusivity/($m^2 s^{-1}$)
A_r	Aspect ratio, $A_r = H\ L^{-1}$/(−)
c_k	Particle speeds/(m s^{-1})
c_s	Lattice speed of sound/(m s^{-1})
f	Distribution function/(kg m^{-3})
f^{eq}	Equilibrium distribution function/(kg m^{-3})
f^{s}	Symmetrical distribution function/(kg m^{-3})
f^{a}	Asymmetrical distribution function/(kg m^{-3})
f^{seq}	Symmetrical equilibrium distribution function/(kg m^{-3})
f^{aeq}	Asymmetrical equilibrium distribution function/(kg m^{-3})
H	Height of the cavity/(m)
L	Length of the cavity/(m)
Nu	Local Nusselt number/(−)
$\overline{Nu}$	Mean Nusselt number/(−)
Pr	Prandtl number $Pr = \nu a^{-1}$/(−)
Ra	Rayleigh number $Ra = g\beta(T_h - T_c)L^3\nu^{-1}a^{-1}$/(−)
t	Time/(s)
t_0	Time scale/(s)
Δt	Time step in lattice Boltzmann equation/(s)
T	Temperature/(K)
T_c	Temperature of the cold wall/(K)
T_h	Temperature of the hot wall/(K)
$u\ v$	Velocities components/(m s^{-1})
$U\ V$	Dimensionless analogues of u, v/(−)
V_{nc}	Velocity scale/(m s^{-1})
$x\ y$	Coordinates/(m)
$X\ Y$	Dimensionless analogues of x, y/(−)
w_k	Weighting factor/(−)

Greek symbols

α	Heat transfer coefficient/(W m^{-2} K^{-1})
β	Coefficient of thermal expansion/(K^{-1})
Θ	Dimensionless temperature/(−)
λ	Heat conductivity coefficient/(W m^{-1} K^{-1})
Λ	Magic parameter/(−)
ν	Kinematic viscosity/($m^2 s^{-1}$)
ρ	Density/(kg m^{-3})
τ	Dimensionless time/(−)
ω_s	Symmetrical relaxation rate/(s^{-1})
ω_a	Asymmetrical relaxation rate/(s^{-1})

✉ Alexander Nee
nee_alexander@mail.ru

Ali J. Chamkha
a.chamkha@kcst.edu.kw

[1] Research and Educational Center of I.N. Butakov, National Research Tomsk Polytechnic University, Tomsk, Russia

[2] Faculty of Engineering, Kuwait College of Science and Technology, Doha District, Kuwait

[3] Center of Excellence in Desalination Technology, King Abdulaziz University, P.O. Box 80200, Jeddah 21589, Saudi Arabia

Introduction

Turbulent buoyancy-driven flows are encountered in different engineering problems such as Trombe wall, electronics and fuel cell cooling, building thermophysics and solar collectors. In order to examine thermal and flow regularities, mathematical physics methods are predominantly applied since an up-to-date experimental study of turbulent convection is very expensive. However, despite some progress in simulation of turbulent flows an accurate turbulence modeling is still a great challenge.

Nowadays, Reynolds averaged Navier–Stokes (RANS) approach [1–4] is mainly used to simulate turbulent buoyancy flows. Popularity of this approach is due to an acceptable time of computation. Along with that speed up in computation reduces accuracy. Moreover, RANS models are semiempirical. Consequently, results obtained with these models should always be validated by experimental data. On the contrary, classical macroscopic direct numerical simulation (DNS) provides accurate results [5–9] without any additional information. But this accuracy requires massive computation resources and time. On the other hand, mesoscopic lattice Boltzmann method (LBM) can successfully deal with this kind of problems as shown in [10]. The most relevant studies are presented below.

One of the first attempts to utilize lattice Boltzmann method to perform a direct numerical modeling of high Rayleigh number flow in a cavity heated from the side was done by Dixit and Babu [10]. The authors used widely accepted LBGK model to examine the thermal and flow fields in a range of the Rayleigh number $10^4 \leq Ra \leq 10^{10}$. However, it is well known that standard Bhatnagar–Gross–Krook approximation suffers numerical instabilities with high Rayleigh number flows. So, to overcome this weakness, Dixit and Babu applied interpolation supplemented technique and computations were performed on a non-uniform mesh. To increase numerical stability, multiple relaxation time (MRT) approximation can be used instead of simple BGK model. Du and Liu [11] studied buoyancy-driven flow via MRT LBM with eight-by-eight collision matrix. The eight velocity directions were applied in the velocity space. Mathematical modeling was conducted for air with $10^3 \leq Ra \leq 10^9$. A two-population entropic MRT lattice Boltzmann simulation was performed in [12]. Frapolli et. al. considered both the canonical non-rotating and rotating turbulent Rayleigh–Bénard convection.

Another approach to apply LBM for high Rayleigh number flows is to perform relaxation of central moments in a "cascaded manner." This model is known as cascaded lattice Boltzmann (CLBM). Sharma et. al. [13] tested CLBM on a benchmark problem of natural convection in a closed square cavity in a range of $10^3 \leq Ra \leq 10^{10}$. It was found that the wall shear stresses and the Nusselt numbers were satisfactory agreed with the DNS and experimental data.

In order to conduct lattice Boltzmann modeling on non-uniform and curvilinear grids, Polasanapalli and Anupindi [14] extended a compact finite difference lattice Boltzmann method (CFDLBM). The authors studied buoyancy-driven flows in square and concentric circular annulus cavities with the Rayleigh number up to 10^9.

In the studies presented above, passive scalar approach (PSA) was used as a thermal model. Moreover, DNS based on the lattice Boltzmann equation was predominantly performed for $Ra \leq 10^{10}$. It should be stressed that Lallemand and Luo [15] noted that a hybrid approach had a higher numerical stability in comparison with PSA in some cases. Thus, the aim of this work is to examine the capability of hybrid lattice Boltzmann method to simulate high Rayleigh number flows up to 10^{11}.

Problem statement

It is general practice to implement the Reynolds averaged Navier–Stokes technique to study turbulent flow patterns. However, it needs to be stressed that RANS was originally developed to examine forced convection. Hence, a significant error can arise when implementing RANS for buoyancy-driven flows. Therefore, we adopted the pseudo-direct numerical simulation (pDNS) technique in order to obtain reliable results. However, it is well known that the conventional DNS approach is computationally very expensive and numerical implementation of high-order finite difference schemes is a big challenge. So we used alternative lattice Boltzmann method to compute the flow field. But general LBGK model suffers numerical instabilities with high Rayleigh numbers. To increase stability of the LBM, we applied two-relaxation time approximation and the hybrid formulation with implicit solution of energy equation. The great benefit of the proposed hybrid pseudo-direct numerical simulation over RANS and LES is no need for empirical input data. Consequently, the pDNS can be considered as a universal CFD tool both for laminar and turbulent flow behavior analysis.

Pseudo-direct numerical simulation of high Rayleigh number flow was performed for a differentially heated cavity with different aspect ratios (Fig. 1). Pseudo-direct numerical simulation (pDNS) is a CFD technique similar to conventional direct numerical simulation (DNS). When performing the DNS, Kolmogorov scales of time and space must be fully resolved. On the contrary, these scales can partially be unresolved under pDNS [16–18]. This factor significantly lightens the computational load, and a solution is obtained much more faster in comparison with pure DNS. It should

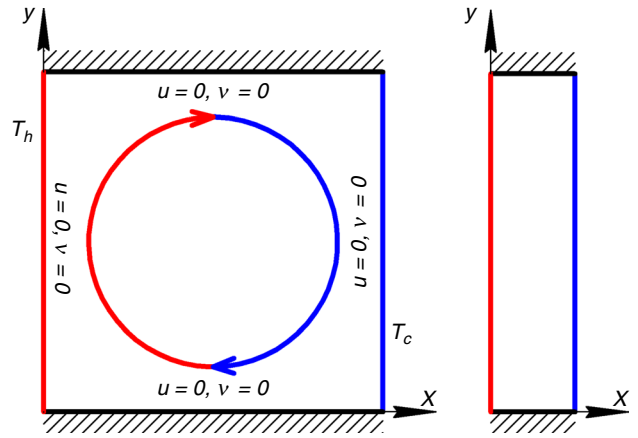

Fig. 1 Solution domain: $a - A_r = 1$; $b - A_r = 4$

be stressed that physical dissipation effects are introduced through the numerical viscosity. Thus, very important issue is the choice of convective terms approximation scheme.

The problem statement assumes that physical parameters such as thermal diffusivity and heat conductivity are temperature-independent. Low Mach number two-dimensional transient flow under Boussinesq approximation is studied. The Dirichlet conditions are set at the vertical walls, whereas horizontal boundaries are assumed to be heat insulated. The fluid is considered as an absolutely transparent medium for thermal radiation.

Two-relaxation time lattice Boltzmann formulation

In the present study, the two-relaxation time (TRT) proposed by Ginzburg [19] is applied to approximate a collision operator in the Boltzmann equation. The TRT is a kind of compromise between the single relaxation time (SRT) and the multiple relaxation time approximations. On the one hand, numerical stability of the TRT is superior to the SRT. On the other hand, numerical implementation of the TRT is not as complicated as the MRT. The discretized mesoscopic lattice Boltzmann equation under the TRT approximation and the D2Q9 scheme with buoyancy force term is as follows:

$$f_k\left(\vec{x}+\vec{c}_k\cdot\Delta t,\ t+\Delta t\right)=f_k\left(\vec{x},\ t\right)-\Delta t\cdot\omega_s\cdot\left(f_k^s-f_k^{seq}\right)-\Delta t\cdot\omega_a\cdot\left(f_k^a-f_k^{aeq}\right)+\Delta t\cdot F. \tag{1}$$

where $k = 1.0.9$. In the collision side, the distribution function f is divided into the symmetrical f^s and asymmetrical f^a parts with corresponding relaxation rates. The symmetrical relaxation rate ω_s is related to shear viscosity, and the asymmetrical relaxation rate ω_a is related to energy fluxes [20].

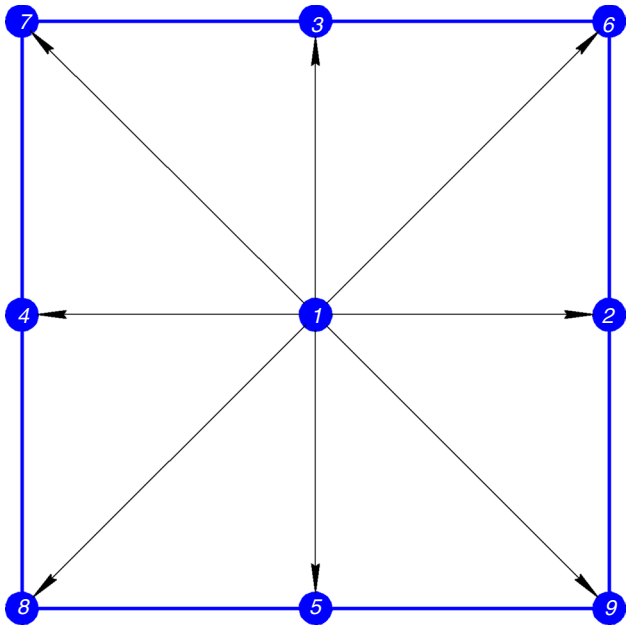

Fig. 2 D2Q9 scheme

The symmetrical and asymmetrical distribution functions can be expressed as follows:

$$f_k^s=\frac{f_k+f_{-k}}{2},\ f_k^{seq}=\frac{f_k^{eq}+f_{-k}^{eq}}{2},\qquad f_k^a=\frac{f_k-f_{-k}}{2},\ f_k^{aeq}=\frac{f_k^{eq}-f_{-k}^{eq}}{2}. \tag{2}$$

where $f_k^{eq}=w_k\cdot\rho\cdot\left[1+\frac{c_k\cdot u}{c_s^2}+\frac{(c_k\cdot u)^2}{2\cdot c_s^4}-\frac{u^2}{2\cdot c_s^2}\right]$ is the equilibrium distribution function; w_k is the weights: $w_1 = 4/9$, $w_{2..5} = 1/9$, $w_{6..9} = 1/36$; ρ is density; c_k is particle speeds: $c_1 = (0, 0)$, $c_{2..5} = (\pm1, 0), (0, \pm1)$, $c_{6..9} = (\pm1, \pm1)$; c_s is lattice speed of sound; and $-k$ is the counter direction of k (Fig. 2). If k is equal to 2, then the counter direction is 4. Analogously, the counter direction for $k = 6$ is $-k = 8$, etc.

Macroscopic variables such as density and velocity are related to the distribution function as:

$$\rho=\sum_{k=1}^{9}f_k, \tag{3}$$

$$u=\frac{1}{\rho}\cdot\sum_{k=1}^{9}c_k\cdot f_k. \tag{4}$$

The symmetrical relaxation rate is computed through the kinematic viscosity as:

$$\omega_s = \frac{c_s^2 \cdot \Delta t}{\nu + 0.5 \cdot c_s^2 \cdot \Delta t}, \tag{5}$$

It is known that the best numerical stability is obtained with the $\Lambda = 0.25$.

The buoyancy force in Eq. (1) can be determined as follows:

$$F = 3 \cdot \rho \cdot w_k \cdot c_y \cdot g \cdot \beta \cdot \left(T - \frac{T_h + T_c}{2}\right). \tag{6}$$

where g is acceleration due to gravity; β is volumetric thermal expansion; T_h is temperature of the hot wall; and T_c is temperature of the cold wall.

A simple bounce back condition is implemented to define the value of the distribution function at the walls.

Heat transfer formulation

In this study, the lattice Boltzmann method is coupled with a macroscopic energy equation in order to analyze thermal behavior of turbulent flow. The dimensionless energy equation under conditions of natural convection is as follows:

$$\frac{\partial \Theta}{\partial \tau} + U\frac{\partial \Theta}{\partial X} + V\frac{\partial \Theta}{\partial Y} = \frac{1}{\sqrt{\mathrm{Ra} \cdot \mathrm{Pr}}}\left(\frac{\partial^2 \Theta}{\partial X^2} + \frac{\partial^2 \Theta}{\partial Y^2}\right). \tag{7}$$

where $Ra = \frac{g \cdot \beta \cdot (T_h - T_c) \cdot L^3}{\nu \cdot a}$ is Rayleigh number; $\mathrm{Pr} = \frac{\nu}{a}$ is Prandtl number; and a is thermal diffusivity, $\mathrm{m^2 s^{-1}}$.

The following conditions are set for Eq. (7):

$$\Theta(X, Y, \tau = 0) = \frac{\Theta_h + \Theta_c}{2} = 0.5, \tag{8}$$

$$U(X, Y, \tau = 0) = V(X, Y, \tau = 0) = 0, \tag{9}$$

$$0 < X < 1: \quad \left.\frac{\partial \Theta}{\partial Y}\right|_{Y=0, Y=1} = 0, \tag{10}$$

$$X = 0,\ 0 < Y < 1: \ \Theta = 1, \tag{11}$$

$$X = 1,\ 0 < Y < 1: \ \Theta = 0, \tag{12}$$

The following relations are applied to make Eq. (7) with initial (8), (9) and boundary (10)–(12) conditions dimensionless:

$$X = \frac{x}{L};\ Y = \frac{y}{L};\ U = \frac{u}{V_{nc}};\ V = \frac{v}{V_{nc}};\ \Theta = \frac{T - T_c}{T_h - T_c};\ V_{nc} = \sqrt{g \cdot \beta \cdot (T_h - T_c) \cdot L}. \tag{13}$$

The heat transfer rate is estimated in terms of the local and mean Nusselt numbers as:

$$Nu_h = \left.\frac{\partial \Theta}{\partial X}\right|_{X=0},\ Nu_c = \left.\frac{\partial \Theta}{\partial X}\right|_{X=1}, \tag{14}$$

$$\overline{Nu_h} = \int_0^1 \left.\frac{\partial \Theta}{\partial X}\right|_{X=0} dY,\ \overline{Nu_c} = \int_0^1 \left.\frac{\partial \Theta}{\partial X}\right|_{X=1} dY \tag{15}$$

The partial differential Eq. (7) is discretized by the finite difference technique. The first- and second-order schemes are applied to approximate temporal and convective terms. Diffusive terms are discretized by the central differences. Difference analogues obtained after discretization are solved by means of the sweep method.

Results and discussion

Numerical prediction of turbulent buoyancy-driven flow patterns is performed in a wide range of governing parameters. The cavity aspect ratio A_r is changed from 1 to 4. Computations are conducted for the Rayleigh number range of $10^9 \le Ra \le 10^{11}$ with the fixed Prandtl number of $\mathrm{Pr} = 0.71$ corresponding to air. Results of numerical simulations are presented in terms of the temperature and streamline contours, streamslices, temperature and velocity profiles, local and mean Nusselt numbers.

Square cavity with $A_r = 1$

Firstly, the classical benchmark problem of turbulent free convection in a square air-filled cavity is considered. It is known that the flow behavior becomes turbulent when the $Ra = 2 \cdot 10^8$. Thus, simulations are performed in a range of $10^9 \le Ra \le 10^{10}$.

Before the main numerical procedure, grid convergence should be checked. In particular, this issue is crucial when applying the pseudo-DNS approach. Figures 3 and 4 show temperature, streamlines, vector fields and magnitude of velocity $\left(W = \sqrt{U^2 + V^2}\right)$. The isotherm step is 0.05.

It is found that a uniform thermal stratification filled almost the entire cavity with the number of 501^2 nodes. Probably, only large eddies are resolved with this mesh size. It should be stressed that the numerical solution obtained with the proposed hybrid TRTLB–FD approach is similar to those computed by RANS models [1–4]. On the other hand, the isotherm configuration is drastically altered when increasing the mesh size to 601^2. Temperature oscillations are clearly observed and fluctuations are found at the left

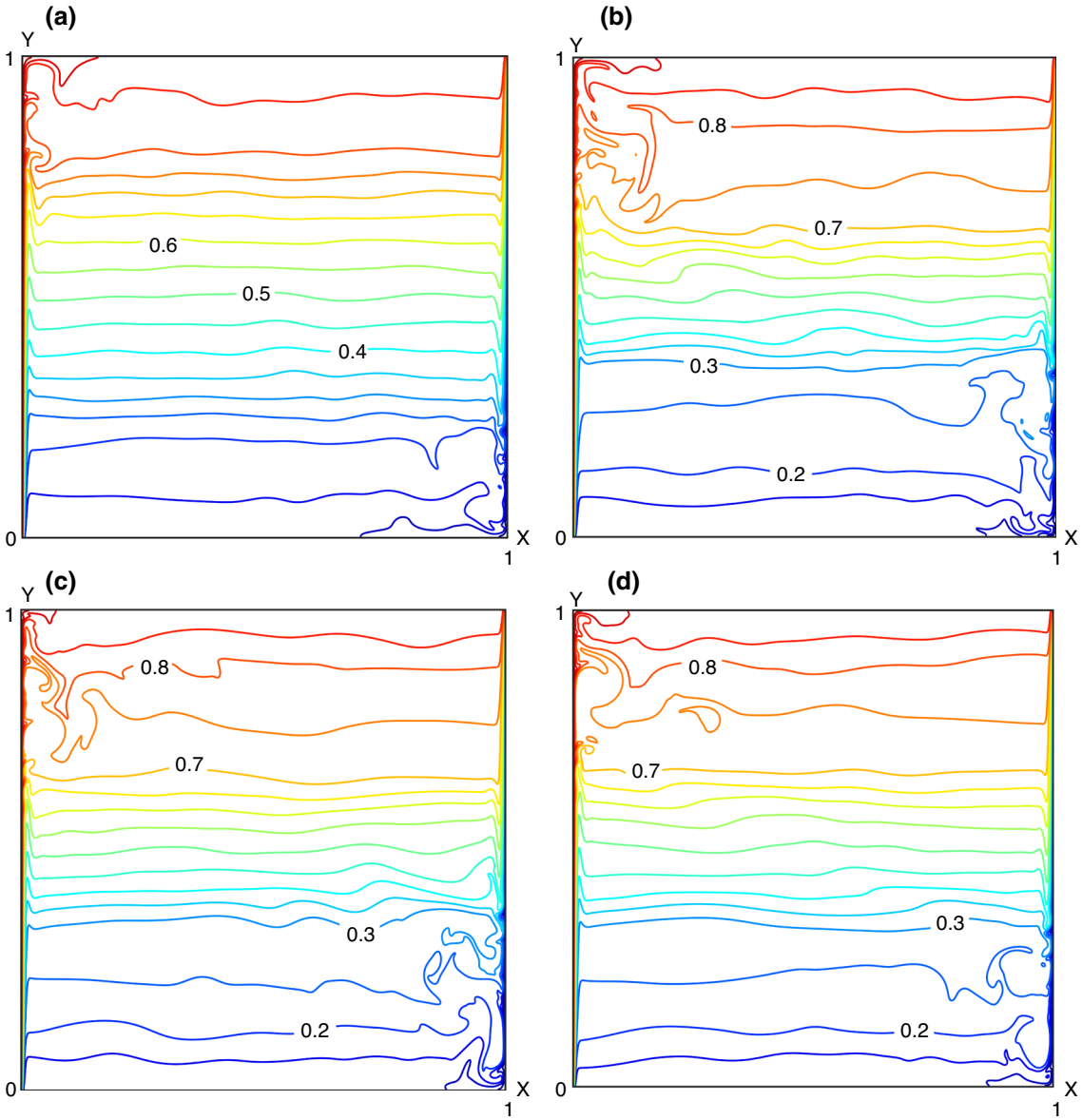

Fig. 3 Temperature contours when $Ra = 10^{10}$ and $\tau = 1000$: **a** 501^2, **b** 601^2, **c** 701^2, **d** 801^2

top and right bottom corners of the cavity. In addition, the temperature is reduced in the areas of $0 < X < 1$, $0.2 < Y < 0.4$, $0.6 < Y < 0.8$ (Fig. 3b). A further increment in the number of nodes slightly affects the thermal field in the core of the analysis domain. The isotherm shape is insignificantly changed near the isothermal walls. Finally, the quasi-grid-independent solution is obtained with the grid size of 701^2. The isotherm location is almost identical when comparing the temperature contours with 701^2 and 801^2 nodes. The near-wall behavior is also similar. Figure 4 represents the streamlines with the variation of mesh size.

A complex flow structure is observed inside the square cavity due to turbulent flow behavior. As could be expected, the flow pattern is altered every time with variation of the grid size. When examining the vector fields and contours of velocity magnitude, it can be stated that laminar and turbulent boundary layers simultaneously exist at the isothermal walls. The highest values of velocity are found at the top left and bottom right corners of the solution domain. Along with that, there is almost no circulation at the core of the cavity. More small-scale structures are resolved as the number of grid points is increased. However, a noticeable alteration of heat transfer and fluid flow patterns is observed between the mesh sizes of 501^2 and 601^2. A quasi-grid-independent solution in terms of the temperature is obtained when the number of nodes is equal to 701^2. Consequently, the thermal field remains almost the same, whereas the flow pattern is changed. This could be possible when the magnitude

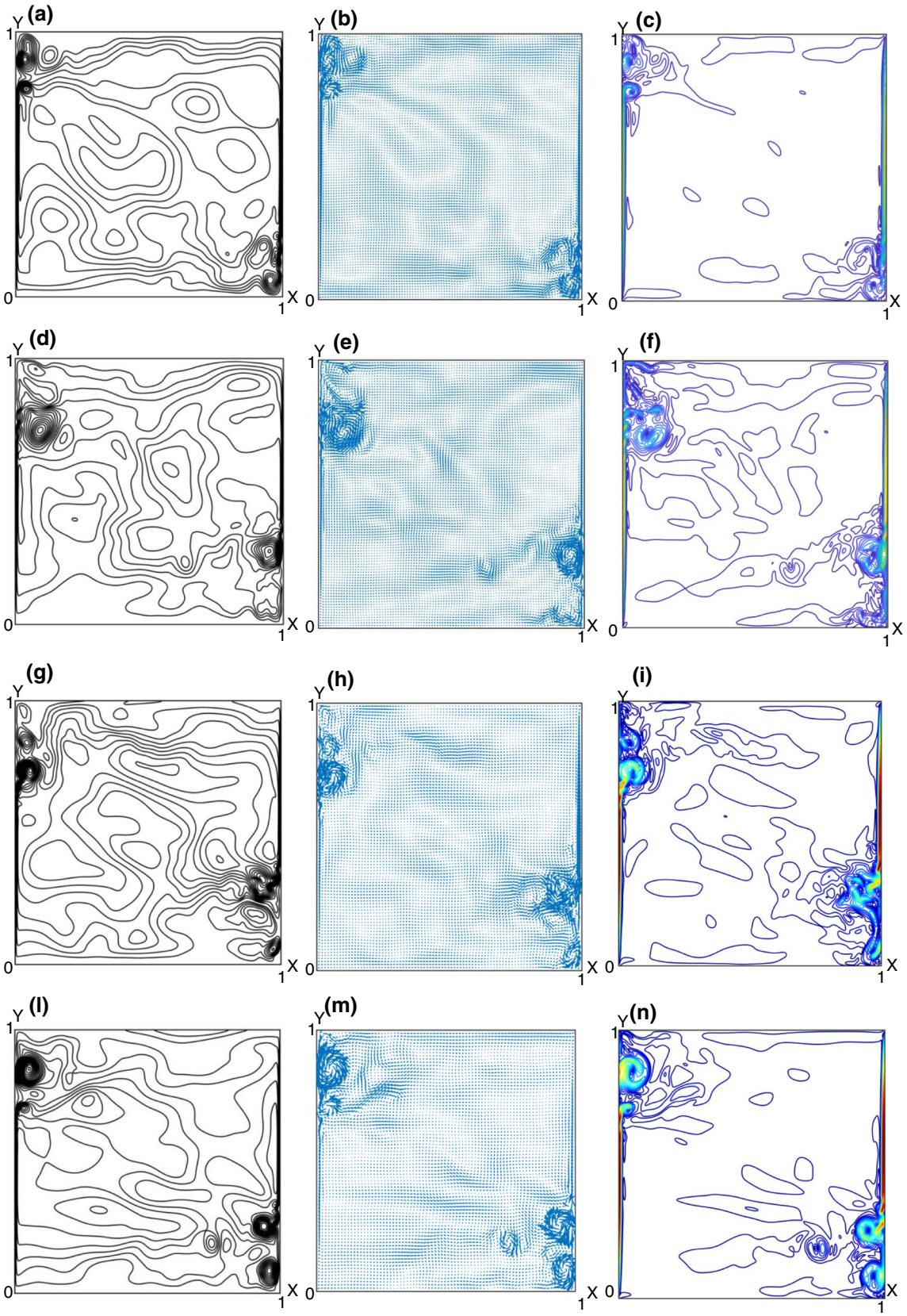

Fig. 4 Streamlines **a**, **d**, **g**, **l**, vector fields **b**, **e**, **h**, **m** and velocity magnitude **c**, **f**, **i**, **n** when $Ra = 10^{10}$ and $\tau = 1000$: **a**, **b**, **c** 501^2, **d**, **e**, **f** 601^2, **g**, **h**, **i** 701^2, **l**, **m**, **n** 801^2

Table 1 Mean Nusselt numbers and CPU times when $Ra = 10^{10}$ and $\tau = 1000$

Grid size	501^2	601^2	701^2	801^2
$\overline{Nu_H}$	82.64	87.69	90.57	89.68
$\overline{Nu_C}$	82.44	88.94	90.07	89.55
CPU times/h	68.8	92.49	155.86	205.67

of velocity fluctuations is insignificant. That hypothesis is proved by distributions of velocity vectors. Variation of the mean Nusselt numbers at the isothermal walls along with the CPU times is presented in Table 1.

The mean Nusselt number is significantly increased for both the hot and cold isothermal walls with an increment in the number of nodes from 501^2 to 601^2. However, a deviation in the mean Nusselt numbers of less than 1% is achieved between 701^2 and 801^2. Thus, at least the grid size of 701^2 should be applied to study the thermal and turbulent flow patterns in closed square cavities by the hybrid TRTLB–FD model when $Ra \leq 10^{10}$. CPU times are of interest since we perform pseudo-direct numerical simulation. In order to perform computations, we have involved a computer class equipped by 10 PC with Intel Core i3-8100 CPUs and 4 GB of DDR4 RAM. CPU times were estimated by means of the "tic-tok" function of MATLAB. The numerical codes were run at least three times. The discrepancies in the executed times did not exceed 5%.

Figure 5 shows temperature profiles in the midlength and the local Nusselt numbers at the hot wall of the cavity when varying the Rayleigh number. The benchmark data obtained with cascaded LBM [13] are also presented.

When performing a general observation, it could be stated that an increment in the Rayleigh number leads to a slight increase/decrease of the temperature near the top/bottom wall. This regularity is obviously concerned with the enhancement of the buoyancy force. The local Nusselt numbers at the hot wall are grown for the same reason. A very accurate solution is obtained in terms of the temperature and the local Nusselt numbers with $Ra = 10^9$. However, an insignificant deviation is revealed when increasing the Rayleigh number to 10^{10}. It should be stressed that Sharma et al. [13] presented the time-averaged data. So the error may be reduced when comparing the instantaneous solutions. Table 2 shows the mean Nusselt numbers for the hot wall for different Rayleigh numbers. The benchmark data obtained with different numerical techniques are also presented.

Based on the data presented in Table 2, a reasonable conclusion could be made that the Nusselt numbers obtained with the proposed pseudo-DNS approach are well correlated with the results of other researches except for high Reynolds turbulent viscosity methods [1, 26]. When performing

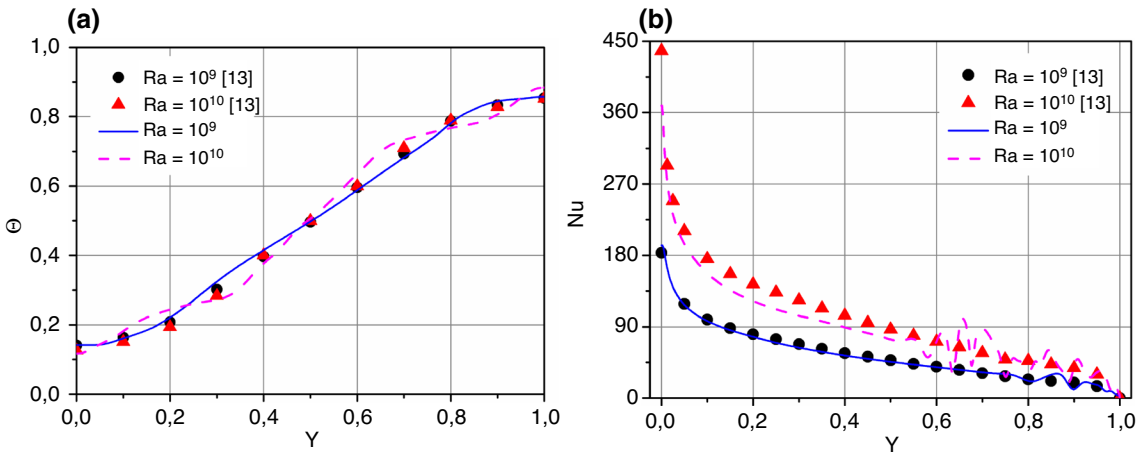

Fig. 5 Temperature **a** and local Nusselt number **b** variation with the Rayleigh number

Table 2 Variation of the *Nu* at the hot wall

Ra	Conventional DNS [23]	FMLBM LES [24]	CDUGKS LBM-based DNS [25]	RANS with standard $k-\varepsilon$ model [1]	Meshless method with Spalart–Allmaras model [26]	Hybrid TRTLB–FD model
10^9	54.6	54.51	52.3	74.96	51.71	53.81
10^{10}	100	98.171	89.49	156.85	149.8	90.57

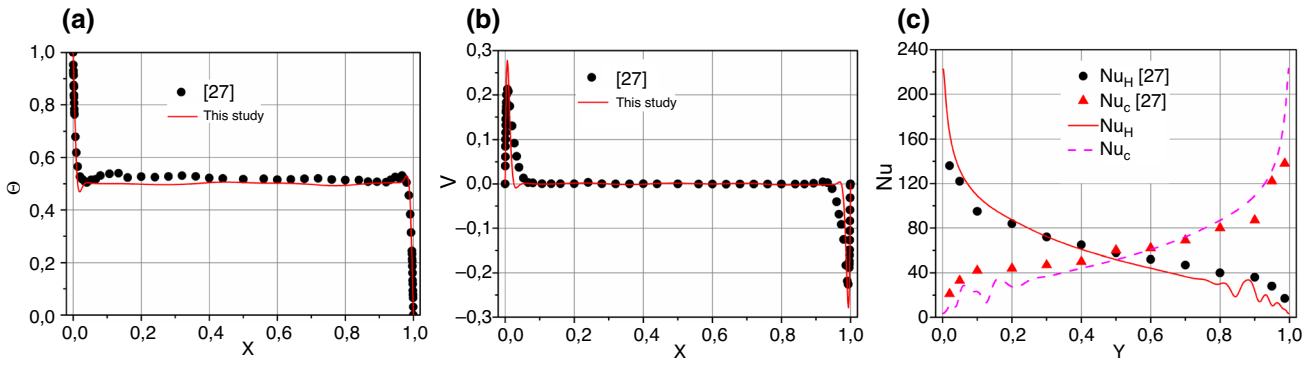

Fig. 6 Variation of temperature **a**, velocity **b** and local Nusselt numbers **c**

a detailed analysis, it is revealed that the error between the "true" conventional direct numerical simulation data [23] and the hybrid TRTLB–FD model does not exceed 1.5% with $Ra = 10^9$. In general, the LBM-based techniques show the similar heat transfer rate results when $Ra = 10^9$. A discrepancy in the mean Nusselt numbers is observed when increasing the buoyancy force. The divergence between the DNS [23] and the proposed hybrid lattice Boltzmann method is around 9% when $Ra = 10^{10}$. On the contrary, the mean Nusselt number computed in this study is in an excellent agreement with the data obtained by the coupled discrete unified gas kinetic scheme [25] even without a grid refinement procedure.

The proposed hybrid pseudo-DNS approach was additionally validated against experimental data of Ampofo and Karayiannis [27]. The authors performed a benchmark study of turbulent thermal convection in a cavity filled with air when $Ra = 1.58 \cdot 10^9$. Figure 6 presents a comparison of temperature, velocity and local Nusselt numbers at the isothermal walls.

When analyzing the data presented in Fig. 6, it is explored that the temperature profile computed with the TRTLB–FD model agrees well with the results of Ampofo and Karayiannis [27]. The same trend of velocity is obtained. However, it should be stressed that a discrepancy in the extremum values is observed (Fig. 6b). Probably, higher values of V are associated with the 2D problem formulation. On the other hand, Ampofo and Karayiannis [27] used a 3D domain where the square plane was considered. Conceivably, the local Nusselt numbers at both at the hot and cold walls are higher for the same reason. But in general, the error is insignificant. Thus, the results of this study are in agreement with the benchmark experimental data.

Tall cavity with $A_r = 4$

When considering turbulent natural convection, tall cavities are often studied. A decrease in the solution domain along

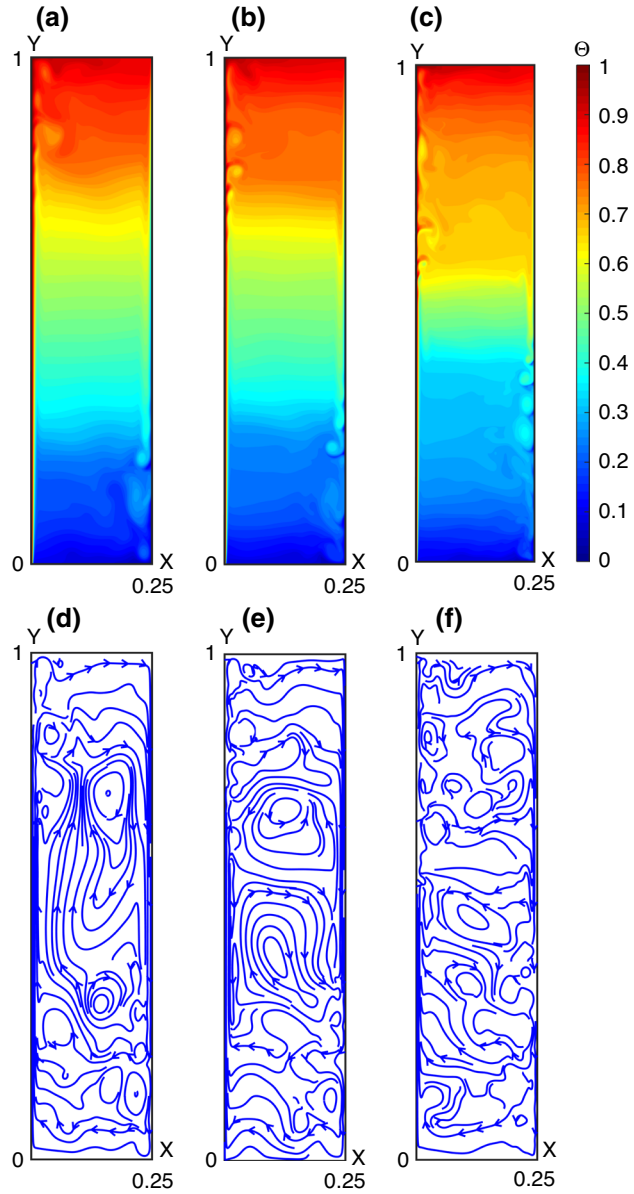

Fig. 7 Temperature contours **a**, **b**, **c** and streamslices **d**, **e**, **f** when: **a**, **d** $Ra = 10^{10}, \tau = 440$; **b**, **e** $Ra = 3 \cdot 10^{10}, \tau = 280$, **c**, **f** $Ra = 10^{11}, \tau = 240$

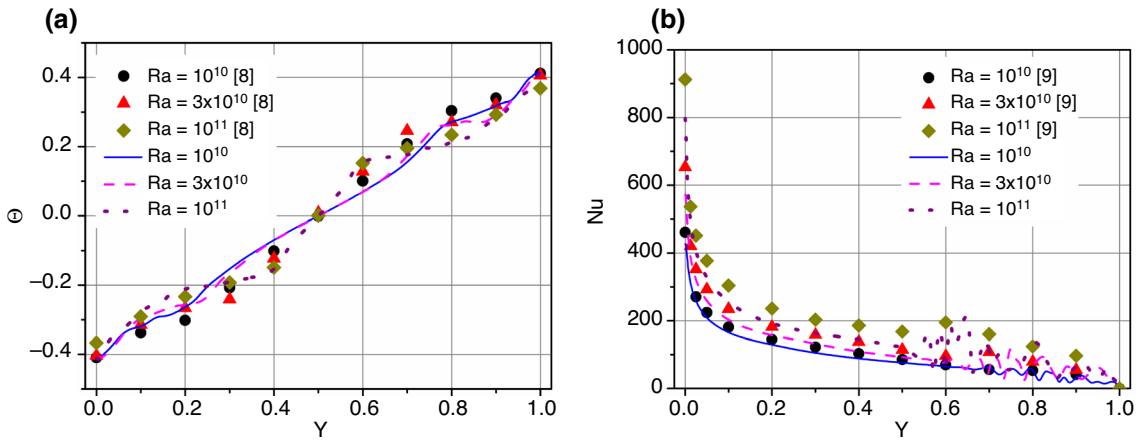

Fig. 8 Variation of temperature **a** in the section of $X=0.125$ and local Nusselt numbers at the hot wall **b**

the X-axis allows reducing the grid size and, consequently, computational resources are saved. Moreover, a quasi-stationary solution is obtained faster in the case of heating from the side. Temperature contours and streamslices for fully developed turbulent flow are shown in Fig. 7.

The thermal field becomes less stratified with an increment in the Rayleigh number. This behavior is concerned with the formation of convective plumes at the isothermal walls. The intensity and number of convective plumes are increased as the buoyancy force is enhanced. These factors lead to a de-stratification. The temperature is lowered/increased in the top/bottom half of the cavity. When analyzing the flow pattern, it is revealed that turbulization significantly affects the secondary currents inside a large-scale convective cell. Small eddies are predominantly formed with an increment in the Rayleigh number. On the other hand, configuration of outer flows near the top walls is slightly altered.

The results of the study are compared with the benchmark DNS data of Trias et al. [8, 9]. Figure 8 presents profiles of temperature and local Nusselt numbers.

In general, satisfactory agreement is observed both for the temperature and the local Nusselt numbers. When performing a careful examination, it is revealed that the proposed hybrid TRTLB–FD model reproduces almost the same trend of temperature profiles with variation of the buoyancy force. Moreover, the best match is achieved in the case of the highest Rayleigh number. On the contrary, a discrepancy in the local Nusselt numbers at the hot wall is increased with an increment in the Rayleigh number since the thickness of the boundary layer at the isothermal walls is decreased. Probably, in order to reduce the error, a grid refinement technique near the solid walls can be applied in the proposed hybrid lattice Boltzmann method. However, a slightly more accurate solution will be obtained, whereas the numerical procedure will become drastically harder. It is interesting to note that the discrepancy in heat transfer rate is reduced as the height of the cavity is increased. Moreover, the TRTLB–FD model accurately predicts the location of the beginning of the local Nusselt number fluctuations along the hot wall even without a mesh refinement procedure.

Conclusions

A very simple approach to study the highly turbulent buoyancy-driven flows in square and tall cavities was proposed. Within this approach, the two-relaxation time lattice Boltzmann method was applied to examine the fluid dynamics, whereas the finite difference solver was used to compute the thermal field. Hybrid method suggested in this study showed incomparably better numerical stability than the widespread single relaxation time approximation. Moreover, numerical implementation of the TRT model is significantly easier in comparison with the multiple relaxation time approximation. It should be also stressed that the two-relaxation time model has only one input argument called “magic” parameter. This parameter has been already well studied. On the other hand, the MRT has more than three free parameters in the case of the two-dimensional nine velocity scheme. Simulation results obtained with an in-house numerical code were compared with the up-to-date numerical and experimental data of other researches. In general, satisfactory agreement was demonstrated both in local and mean heat transfer characteristics. It was found that the proposed hybrid TRTLB–FD model accurately captured thermal plumes at the isothermal walls.

In prospect, parallel implementation of the numerical code developed in this study is of great interest.

Acknowledgements The research was carried out within the framework of Tomsk Polytechnic University Development Program. The

authors are willing to express their thanks to the reviewers for their valuable comments and suggestions.

Author contributions AN conducted numerical experiments and prepared the draft. AJC made the necessary corrections and finalized the manuscript.

Funding None.

Declarations

Conflict of interest The authors declare that they have no known competing financial interests or personal relationships that could have appeared to influence the work reported in this paper.

Availability of data and material The raw data will be provided on a reasonable request.

References

1. Markatos NC, Pericleous KA. Laminar and turbulent natural convection an enclosed cavity. Int J Heat Mass Transf. 1998;27:755–72.
2. Barakos G, Mitsoulis E, Assimacopoulos D. Natural convection flow in a square cavity revisited: Laminar and turbulent models with wall functions. Int J Numer Methods Fluids. 1994;18:695–719.
3. Choi S-K, Kim S-O. Turbulence modeling of natural convection in enclosures: A review. J Mech Sci Technol. 2012;26:283–97.
4. Miroshnichenko IV, Sheremet MA. Turbulent natural convection combined with thermal surface radiation inside an inclined cavity having local heater. Int J Therm Sci. 2018;124:122–30.
5. Paolucci S. Direct numerical simulation of two-dimensional turbulent natural convection in an enclosed cavity. J Fluid Mech. 1990;215:229–62.
6. Fusegi T, Hyun JM, Kuwahara K. Three-dimensional simulations of natural convection in a sidewall-heated cube. Int J Numer Methods Fluids. 1991;13:857–67.
7. Xin Sh, Le Quere P. Direct numerical simulations of two-dimensional chaotic natural convection in a differentially heated cavity of aspect ratio 4. J Fluid Mech. 1995;304:87–118.
8. Trias FX, Gorobets A, Soria M, Oliva A. Direct numerical simulation of a differentially heated cavity of aspect ratio 4 with Rayleigh numbers up to 10^{11} – Part I: Numerical methods and time-averaged flow. Int J Heat Mass Transf. 2010;53:665–73.
9. Trias FX, Gorobets A, Soria M, Oliva A. Direct numerical simulation of a differentially heated cavity of aspect ratio 4 with Rayleigh numbers up to 10^{11} – Part II: Heat transfer and flow dynamics. Int J Heat Mass Transf. 2010;53:674–83.
10. Dixit HN, Babu V. Simulation of high Rayleigh number natural convection in a square cavity using the lattice Boltzmann method. Int J Heat Mass Transf. 2006;49:727–39.
11. Du R, Liu W. A New Multiple-relaxation-time Lattice Boltzmann Method for Natural Convection. J Sci Comput. 2013;56:122–30.
12. Frapolli N, Chikatamarla SS, Karlin IV. Entropic lattice Boltzmann simulation of thermal convective turbulence. Comput Fluids. 2018;175:2–19.
13. Sharma KV, Straka R, Tavares FW. Natural convection heat transfer modeling by the cascaded thermal lattice Boltzmann method. Int J Therm Sci. 2018;134:552–64.
14. Polasanapalli SRG, Anupindi K. A high-order compact finite-difference lattice Boltzmann method for simulation of natural convection. Comput Fluids. 2019;181:259–82.
15. Lallemand P, Lou L-S. Hybrid finite-difference thermal lattice Boltzmann equation. Int J Mod Phys B. 2003;17:41–7.
16. Komen E, Shams A, Camilo L, Koren B. Quasi-DNS capabilities of OpenFOAM for different mesh types. Comput Fluids. 2014;96:87–104.
17. Addad Y, Zaidi I, Laurence D. Quasi-DNS of natural convection flow in a cylindrical annuli with an optimal polyhedral mesh refinement. Comput Fluids. 2015;118:44–52.
18. Komen EMJ, Camilo LH, Shams A, Geurts BJ, et al. A quantification method for numerical dissipation in quasi-DNS and under-resolved DNS, and effects of numerical dissipation in quasi-DNS and under-resolved DNS of turbulent channel flows. J Comput Phys. 2017;345:565–95.
19. Ginzburg I, Verhaeghe F, d'Humieres D. Two relaxation-time lattice Boltzmann scheme: About parameterization, velocity, pressure and mixed boundary conditions. Commun Comput Phys. 2008;3:427–78.
20. Esfahani JA, Norouzi A. Two relaxation time lattice Boltzmann model for rarefied gas flows. Phys A. 2014;393:51–61.
21. d'Humieres D, Ginzburg I. Viscosity independent numerical errors for lattice Boltzmann models: from recurrence equations to "magic" collision numbers. Comp Math Appl. 2009;58:823–40.
22. Bhopalam SR, Perumal DA, Yadav AK. Computation of fluid flow in double sided cross-shaped lid-driven cavities using Lattice Boltzmann method. Eur J Mech B Fluids. 2018;70:46–72.
23. Xin S, Le Quéré P. Numerical simulations of 2D turbulent natural convection in differentially heated cavities of aspect ratios 1 and 4. In: Voke PR, Kleiser L, Chollet JP, Editors. Direct and large-eddy simulation I. Fluid mechanics and its applications, Dordrecht: Springer; 1994. p. 26
24. Zhuo C, Zhong Ch. LES-based filter-matrix lattice Boltzmann model for simulating turbulent natural convection in a square cavity. Int J Heat Fluid Flow. 2013;42:10–22.
25. Wang P, Zhang Y, Guo Z. Numerical study of three-dimensional natural convection in a cubical cavity at high Rayleigh numbers. Int J Heat Mass Transf. 2017;113:217–28.
26. Sheikhi N, Najafi M, Enjilela V. Solving natural convection heat transfer in turbulent flow by extending the meshless local Petrov-Galerkin method. Eng Anal Bound Elem. 2018;93:29–43.
27. Ampofo F, Karayiannis TG. Experimental benchmark data for turbulent natural convection in an air filled square cavity. Int J Heat Mass Transf. 2003;46:3551–72.